SIST 2009

Ultrasonic Thermometry in the Verification of Accurate Displacement Measurements in Laser Interferometry.

By Nnadozie Ezerioha [1, 2]
Supervisor: Horst Friedsam [1]

Abstract
The accuracy of distance and position measurements using current advances in laser interferometry today is hindered by temperature gradients along the path of the laser. These temperature gradients along with other environmental conditions decrease the accuracy of measurement due to their effects on the refractive index of air. However, depending on the location, temporal and spatial temperature variations may be large and thereby require a process that would output real-time data highlighting changes in these physical factors. The average temperature around the laser path is difficult to calculate unless a good and efficient technique that can take into consideration all other physical factors such as humidity, atmospheric pressure and the rate of change of temperature is implemented. This paper highlights the design, calibration and testing of an ultrasound transducer device for micro-scale temperature measurements. Measurements in very stable conditions will be compared with measurements in layered and turbulent conditions to determine the working efficiency as well as robustness of the setup.

[1]Fermi National Accelerator Laboratory

[2]Department of Physics and Engineering, Benedict College

Table of Contents **Page**

Introduction: Fermilab

Fermilab, originally known as the National Accelerator Laboratory, was renamed in 1974 in honor of 1938 Nobel Prize winner Enrico Fermi. The mission of the lab is to advance the understanding of the fundamental nature of matter and energy. Particle acceleration is at the helm of Fermilab's very existence. A particle accelerator basically uses electric fields to control electric particles. Using the electric fields created by electromagnets, "beams" of electrically charged particles are steered and controlled, and over time, accelerated within the particle accelerators at Fermilab. There are a series of accelerators at Fermilab used in a step-by-step process, of which the Tevatron is the largest and final accelerator. At four miles in circumference it is substantially more powerful than any other in the world; second only to the newly constructed Large Hadron Collider (LHC) in Switzerland, and uses superconducting electromagnets as its source of electric field. These accelerators are being used to create collisions of proton and antiproton particles, and to record the results of these high-energy collisions. These experiments are in an attempt, to discover the missing link, in the conditions of matter in the early universe.

Two major components of the Standard Model of Fundamental Particles and Forces were discovered at Fermilab: the bottom quark (May-June 1977) and the top quark (February 1995). In July 2000, Fermilab experimenters announced the first direct observation of the tau neutrino, the last fundamental particle to be observed. Filling the final slot in the Standard Model, the tau neutrino set the stage for new discoveries and new physics with the inauguration of Collider Run II of the Tevatron in March 2001.

However central to all of this, is the ability of physicists to control the beams, such that the collisions are best. Even further, being able to control the beam suggests ideal electric fields, which in turn suggests proper magnet alignment. Of course there would also be the appropriate computer programs, and alignment algorithms to control these alignments from a remote location. This paper highlights the design, calibration and testing of an ultrasound transducer device for micro-scale temperature measurements. This will enable high precision measurements by laser interferometers used at Fermilab for alignment work. Measurements in very stable conditions will be compared with measurements in layered and turbulent conditions to determine the working efficiency as well as robustness of the setup.

Overview

Change in the speed of light or the refractive index is a value that must be considered for precision measurements with a laser tracker system. Laser trackers are currently equipped with a system for measuring the ambient temperature and air pressure. Slow changes in these factors are measured and compensated for automatically. However, sudden changes in ambient temperature cannot be noticed yet can have an effect on measurement accuracy. In order to maintain high accuracy, a system that can detect sudden changes in temperature is required. Considering that the speed of sound is affected mostly by temperature than by any other single factor, it is then plausible to equate the change in the speed of sound in the medium of travel to the accuracy of the laser tracker.

Ultrasonic energy has been used in various mechanical applications such as welding, friction reduction, drilling, imaging, physical therapy, and the processing of liquids. The acoustical power used in these applications ranges from just a few watts in laboratory units to several kilowatts in large industrial installations. Almost every segment of industry is a potential user of ultrasonic technology. This does not necessarily mean that a particular solution envisioned through the use of ultrasonic energy is practical. This uncertainty leads to the aim of this project: to test the practicability of the application of ultrasound in micro-scale thermometry.

Light and Sound

The speed of sound is affected by a host of environmental factors including air temperature, pressure, humidity and particles in air. It is also affected by turbulence in the form of air traveling parallel, perpendicular and in opposite directions to it

Theoretically, the speed of sound, c in an ideal gas is represented by;

$$c = \sqrt{\frac{\gamma RT}{\mu}} \qquad \text{Eq. 1}$$

Where R is the ideal gas constant, T is the absolute temperature (in K), and μ is the average molecular weight of the gas molecules. [4]
Because sound needs a medium to propagate, the speed of sound in air is dependent on air itself, its constituents, and behavior at each moment in time.

The Speed of light in a vacuum is approximately 299,792,458 meters per second. This is about 874 thousand times faster than the speed of sound in air: 343 meters per second. This accrues primarily because the speed of sound travel is directly proportional to the density of the particles in its conducting medium hence sound speed in air<speed in liquid<speed in solid; with its speed in aluminum approaching 6,420 meters per second. Because light travels significantly faster than sound, lightning is seen a couple of seconds (depending on the distance of the observer away from the strike) before the sound of thunder is heard. This relationship between the velocities of sound and light, coupled with their dependence on temperature serves as a basis for our research.

Relationship between Sound velocity and temperature

From the previous equation in *Eq. 1.1,* the speed of sound, C $\propto \sqrt{T}$
This implies that the speed of sound (in air in this case) is dependent upon the temperature along or around its travel path. We can thus intrinsically assume that by knowledge of the velocity of sound at every given temperature, which is calculated from distance covered over a given amount of time, ΔT , and by comparing these values with our field data, average temperature along a given path can be calculated.
In theory, speed of sound is independent of pressure p at constant temperature. All other predicted effects of pressure theoretically proven have been shown to be negligible.
As earlier stated, at room temperature the speed of sound is about 345m/sec. As the temperature increases, so does this speed at a defined but imperfectly linear rate that can be calculated with high precision.

Determination of Air Temperature

For the determination of the air temperature, the velocity of sound in air needs to be known. In this case the air can be assumed to be an ideal gas versus a real gas. If the integral temperature is to be determined to less than 0.1 K then sound velocity needs to be known from 0.01 to 0.04 [m/sec]. As air is not a real gas, the sound velocity is dependent on the mixing ration of the individual gas parts with nitrogen (78%) and oxygen (21%) contributing the largest components. Water vapor pressure is another contributing factor in the determination of sound velocity which is usually fluctuating between 1% and 4% of the gas volume. However, the composition of dry air, i.e. 0% relative humidity, can be considered relatively constant and is the basis for the development of the sound velocity formula of an ideal gas:

$$c = \sqrt{\frac{(405.92 - 0.0124T)T}{1 - 0.378(\frac{e}{p})}} \qquad \text{Eq. 2}$$

In this equation the temperature T is given in Kelvin [K]; {T= (273.15+t) with T [K] and t [°C]} while the partial vapor pressure *e* and the air pressure *p* are entered in [hPa]. Using this formula and assuming dry air, one obtains the sound velocity at 0 [°C] to be 331.59 [m/sec] and 343.41 [m/sec] at 20 [°C]. The sound velocity is determined primarily by the temperature and only secondarily by the partial water vapor pressure. The effects of the partial water vapor pressure on the speed of sound increases with increasing temperature while the air pressure can usually be seen as constant for reasonable small measurement intervals.

Under these circumstances, the above formula can be replaced by an approximation for dry air giving:

$$c = 20.0467\sqrt{(273.15 + t)} \qquad \text{Eq. 3}$$

This is further developed by expanding the root in a Taylor series with respect to t, into the following convenient formula for the speed of sound in dry air:

$$c \approx 331.32 + 0.61t \qquad \text{Eq. 4}$$

In this equation *t* is to be entered in [°C] to obtain the velocity of sound in [m/sec]. As one can see a temperature change of 1 [° C] results in a 0.61 [m/sec] change in the speed of sound. This relative strong dependence of the speed of sound to temperature makes this an ideal tool for determining the integral ambient air temperature.

Besides these parameters the speed of sound is also affected by the frequency of the sound waves i.e. dispersion. This effect however is relatively small, and on the order of 0.1 [m/sec]. Considering the air to be a real gas and utilizing the van der Waal equations for ambient air close to the ground, one can derive the following formula for the determination of the speed of sound in dry air:

$$c = \sqrt{-349.29 + 406.965T - 0.0124\,T^2} \qquad \text{Eq. 5}$$

The temperature *T* has to be inserted in [K] to obtain the speed of sound as [m/sec]. For 0 [°C] one obtains a speed of sound of 331.49 [m/sec]. This theoretical value is in good agreement with experimental results obtained by George S. K. Wong and others in 1986 that determined the speed of sound of air to be 331.29 [m/sec].

Considering the relative humidity of air, the above formula is expanded to:

$$c = 20.0533\sqrt{\frac{T}{1 - 0.378(\frac{e}{p})}} \qquad \text{Eq.6}$$

Using this formula, the uncertainty of the calculated speed of sound is estimated to be between 0.01 [m/sec] and 0.04 [m/sec] considering the uncertainty in determining the environmental parameters including the mixing ratios of the gas components.

Measuring the time traveled by an ultra sound pulse over a known distance, one can determine the virtual temperature or in case the partial water vapor pressure is known, the thermodynamic temperature of the air along the ultra sound path. Solving for *t* results in:

$$\frac{(1 - 0.378\left(\frac{e}{p}\right))c^2}{20.0533} - 273.15 = t \qquad \text{Eq.7}$$

With *t* in [°C] and the distance and time travelled measured quantities to determine *c*; whereby

c = distance/ (delta time).

$$[1 - 0.378\left(\frac{e}{p}\right)]\left(\frac{D}{M}\right)^2 - 5477.559 = 20.0533t$$

Eq. 8

Where *D* is the measured distance in meters and *M* the time it takes the sound wave to cross the distance between the emitter and reflector once. Using this formula one can derive the error estimate for the achievable temperature measurement assuming that the distances can be measured to the micron level (10^{-6} m) and *e* and *p* are error free.

$$\left[1 - 0.378\left(\frac{e}{p}\right)\right] = r \qquad \text{Eq. 9}$$

$$r\left(\frac{D}{M}\right)^2 = 20.0533\,T \qquad \text{Eq. 10}$$

Below are diagrams showing the relationships between speed of sound and humidity with respect to temperature.

Graph:

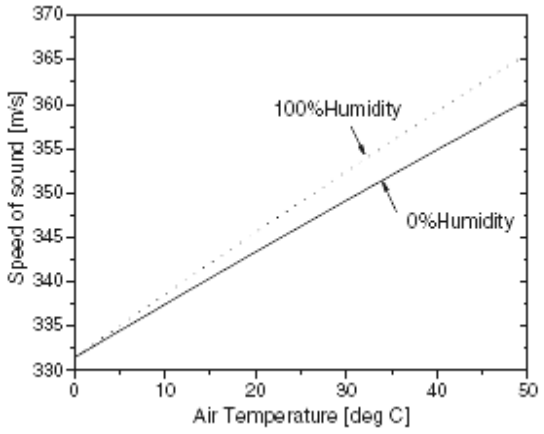

Figure 1. The speed of sound in air as a function of air temperature at 0% and 100% humidity.[4]

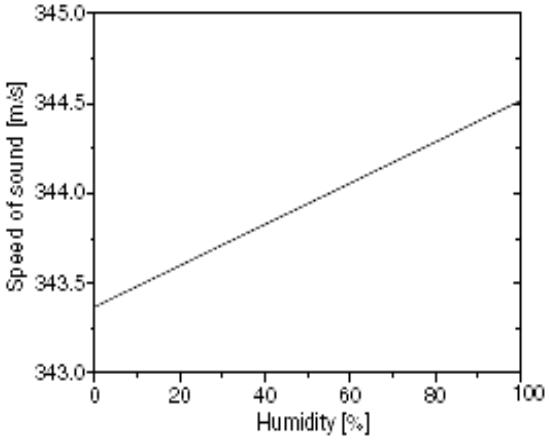

Figure 2. The speed of sound in air at 20 ◦C as a function of humidity.[4]

The Ultrasound transducer

The transducer is the most important part of ultrasound technology. It is the origin of the sound waves and could also be used to detect the echoes as they are reflected back to the source. Several parameters such as width, diameter of transducer as well as its composite material are very instrumental to getting reliable results.

Types: Piezoelectric Transducers

Piezoelectric transducers are primarily employed in the medical industry for imaging of body tissue. They employ piezoelectric elements that convert electrical signals to mechanical forces and vice versa. They all follow a standard model consisting of a capacitor that converts the electrical signals to acoustic waves as shown in the piezoelectric stress equation:

$$S=c^{D}T-hD \qquad \text{Eq 11}$$

Where S is the stress; T is strain; D is the dielectric displacement; c^{D} is the elastic stiffness constant obtained under conditions of constant D, and h is a piezoelectric constant. The piezoelectric element can be thought of as a singing capacitor of area A and thickness d, $C_o=\varepsilon^{s}A/d$ where C_o is the clamped capacitance and s is the clamped (zero strain) dielectric constant. When a voltage, V, is applied across the two electrode faces of the capacitor, oppositely signed stresses appear on these sides through the piezoelectric effect.

Below is a diagram of a piezoelectric transducer with its transmitted plane wave.

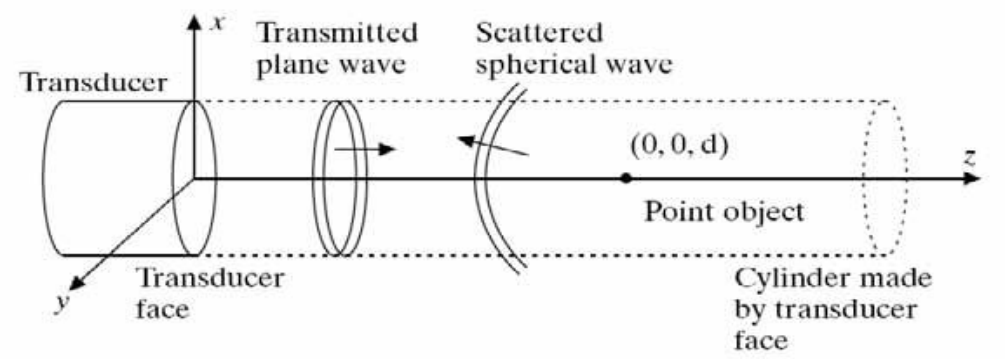

Fig 3. Piezoelectric transducer

Electrostatic Transducers

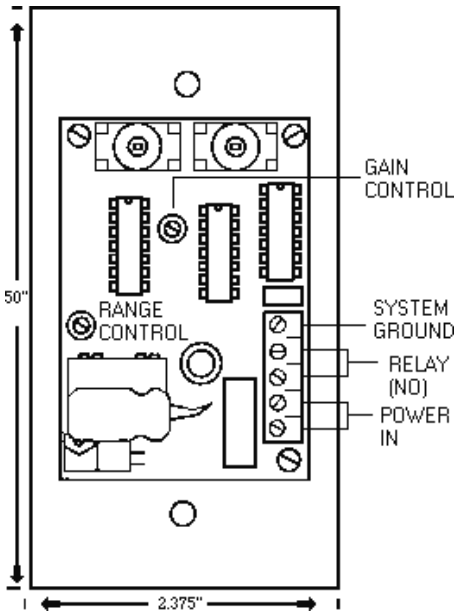

Fig 4. Electrostatic transducer (Sonaswitch 1400 Series)

Output methods

Pulse-Echo Technique

This involves the recording of the time it takes the sound wave to travel the entire distance to the surface of the reflector and back. This is called the Time of flight (TOF). It is measured and halved to give the initial time it takes to reach the reflector surface. The distance between the transducer and the reflector is then divided by this T1/T2 value to give the speed of sound in the medium.

Use of the 53131A Universal Counter

The Hp Agilent 53131A Universal Counter is used for recording TOF as well as Frequency and Period measurements.

Drawbacks

Size: The Sonaswitch transducer was a good model for theoretical purposes but would have been a bad model due to its size and a host of other limiting factors if actually implemented.

During data acquisition, due to the output of a set of 16 pulses, the Universal counter used an averaging function to output an integral of our acquired values every n seconds. This presented a problem for our long-term goals and lead to our seeking a better miniaturized transducer design.

Senscomp Mini A Ultrasonic Transducer

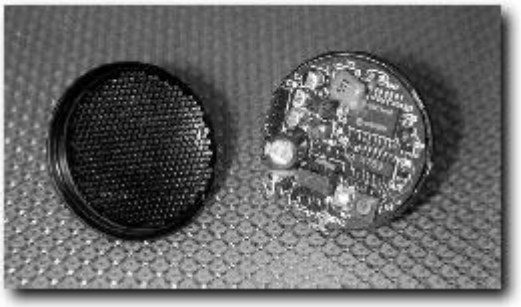

Fig. 5 Senscomp Mini A

The Senscomp Mini-A Ultrasonic Transducer is a 50 KHz electrostatic transducer with integrated SMT electronic circuitry. It has a functional range from 1" to 12", 6" to 20' or from 12" to 40'. It has an Analog output from 0V to 5V and from 0V to 10V depending on the input voltage.
The Analog output value is temperature compensated [based on the temperature of the device]. After much research and experimentation, it was determined that this would actually be of advantage since the transducer components undergo a considerable change in temperature throughout each cycle. It has a +- 0.1% accuracy level over the entire range.

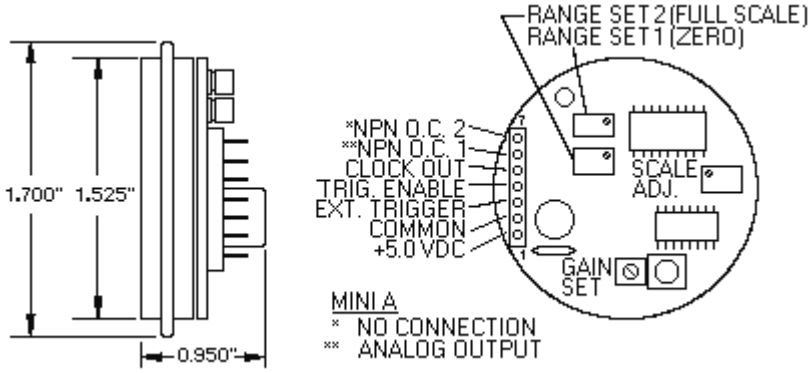

Fig 6. Senscomp Mini A
Courtesy: Senscomp Inc

Transducer Design and Instrumentation
For our planned applications, appropriate design and instrumentation of the transducer was highly required.

Sound Scattering

Large surfaces
Specular – A Specular reflector is a smooth boundary between media (conventional view of reflections. Specular echoes originate from relatively large, regularly shaped objects with smooth surfaces. These echoes are relatively intense and angle dependent.

Small Surfaces

Scattered - Acoustic scattering arises from objects that are the size of sound wavelength or smaller. Echoes originating from relatively small, weakly reflective, irregularly shaped objects are less angle dependant.

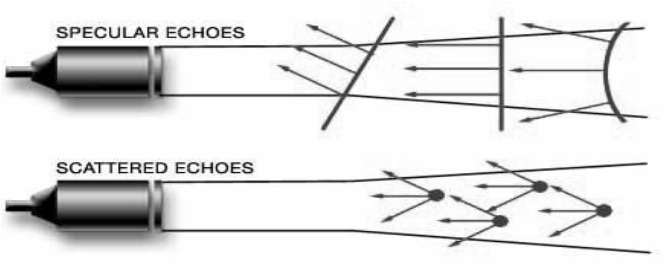

Fig. 7 Sound scattering

For our first round of tests, experiments will be conducted using large surfaces with the reflector directly opposite the source of the sound wave and no angular displacement.

Instrumentation:

A transducer mount was constructed with dimensions 6.000” by 4.000”. A circular groove 1.56” in diameter was made at the (2, 1.5)” point (representing the centre of the transducer). This enabled the setup to be sufficiently shielded from interference by reflections from the ground floor/surface on which it is placed. The mount also contains a 4x4 inch base to provide support and serve as a board for all additional circuitry.

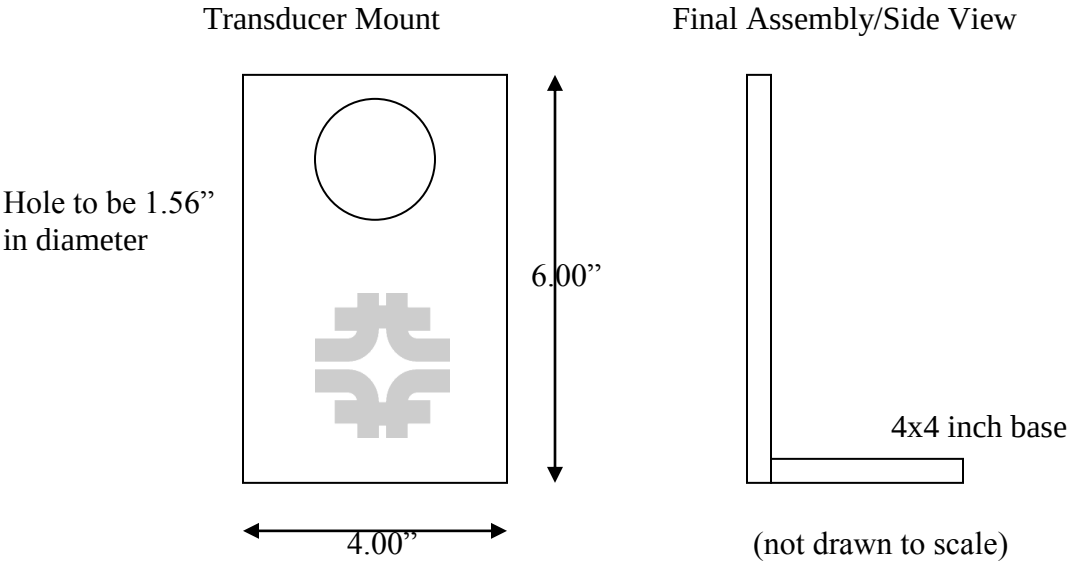

Fig. 8: Transducer Mount

Methods

Calibration:

The Mini A is first calibrated to give a minimum and maximum output at certain predetermined distances. Power is applied through the connector header pin 1. Several minutes are allowed for the Mini A to reach its optimum operating temperature before caliberation. We calculated this to be 3 minutes (minimum). A DC voltmeter's (DVM) Plus(+) lead is connected is connected to the Analog output (pin 6) and the DVM Minus (-) lead to the Common (pin2). The sensor was covered with a stiff piece of flat board. The zero adjust pot was rotated fully counterclockwise. The target was then placed at the desired distance for full scale voltage output. The scale was adjusted until a 5.0 (+) 0.02 VDC reading was obtained. The target was then placed at the desired distance for minimum (zero) voltage output and the zero adjust pot rotated clockwise to 0 (+) 0.31 VDC. Settings were then tested by slowly moving the target from minimum to maximum positions; minor adjustments were then made by first adjusting the full scale pot then the zero-adjust pot. The gain setting was subsequently adjusted to minimum gain for reliable detection.

Initial Calibration Setup

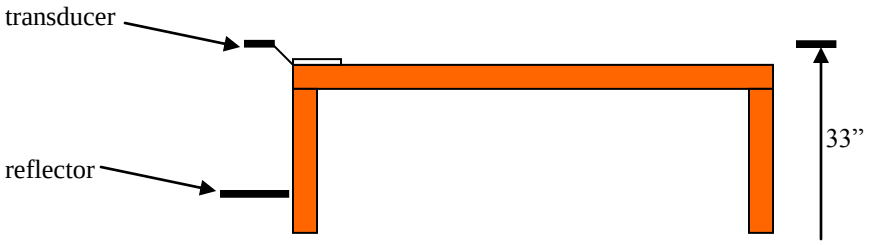

Fig. 9: Calibration

Initial Calibration:

	Distance	**Voltage**
Min	7.5”	0.31v
Max	33”	4.99v

Initial Measurements:

Distance (Inches)	Voltage (V)
0	0.31
7.5	0.31
10	0.42
12	0.846
14	1.282
16	1.649
18	2.016
20	2.492
22	2.759
24	3.21
26	3.59
28	3.98
30	4.31
33	4.99

Table 1.0

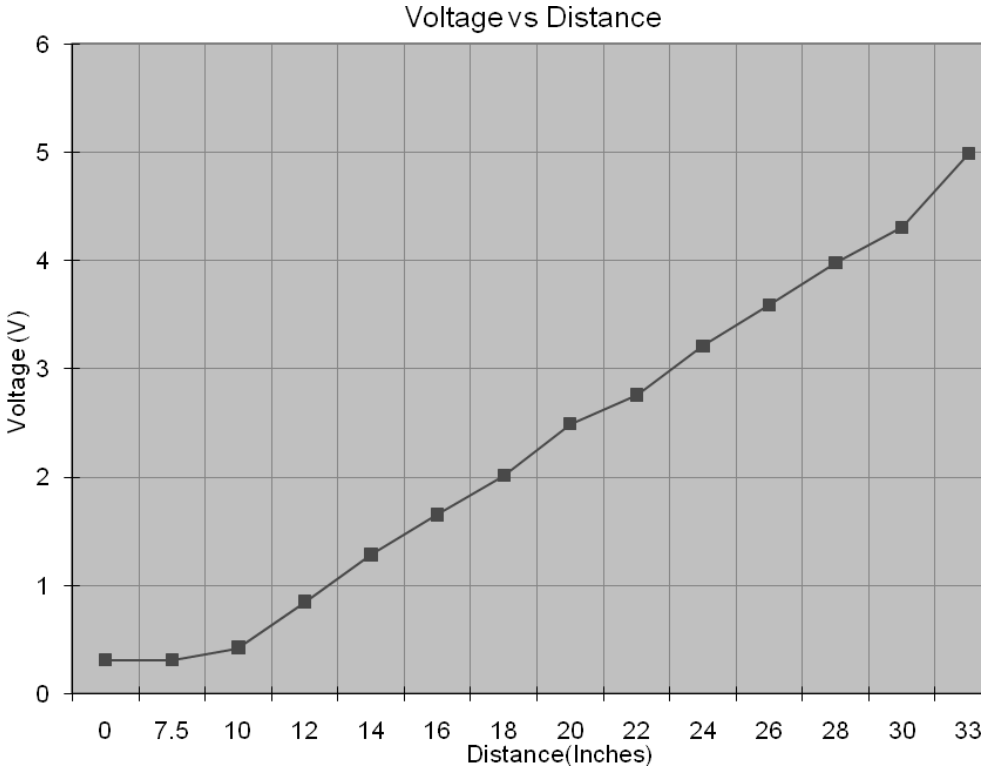

Fig. 10

Above is a graph showing voltage values from the transducer after the 1st calibration plotted over distance

Final Calibration and Testing

After initial calibration and testing, further tests were required on a longer workbench with a fixed-target reflecting surface. The next setup consisted of a tooling bar for accurate distance measurements to the scale of 10^{-5} inches. This enabled us correlate our voltage measurements to distance and calculate the formula required for the conversion, noting temperature changes during each run.

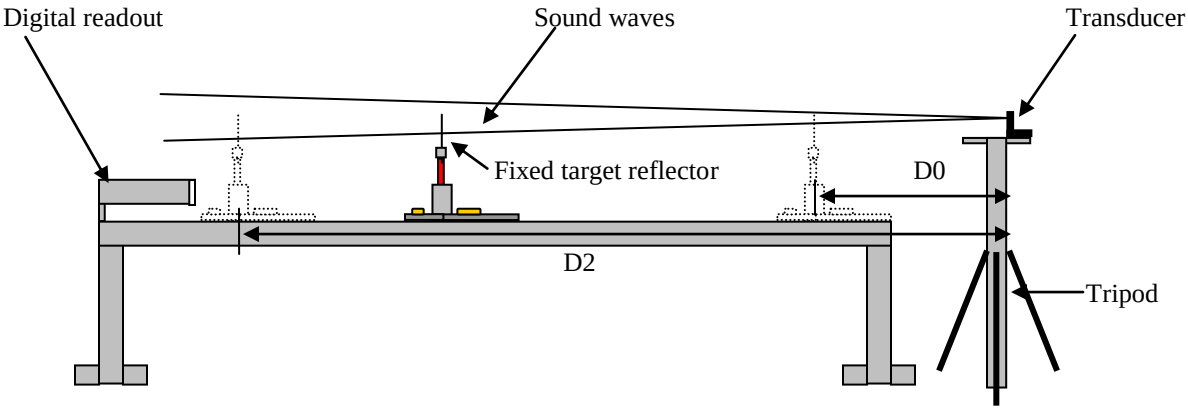

Fig. 11: The Tooling bar Setup

Above is the diagram of the tooling bar with an advanced digital readout to show accurate distance measurements.

Measurements

The Transducer was placed at a stationary point such that the distance D0 =23.75". D0 is the distance between the transducer surface and the reflector surface at minimum distance. D2 refers to the maximum distance between the transducer and the reflector surface. The reflector was placed in the sound-wave field region parallel to the surface of the transducer. This enabled us to record the most accurate measurements.

Positive Pulse Cycle time (PWM Output) = TOF
Velocity of Sound = (D1+D0)/ (TOF/2)

Results

- Run 1.13

Calibrated to work for min: 2 feet, max: 85 inches

Average Value	D1	D0
0.36	0.00	24.00
0.63	5.00	39.00
0.91	10.00	34.00
1.18	15.00	39.00
1.45	20.00	44.00
1.72	25.00	49.00
2.00	30.00	54.00
1.75	35.00	59.00
2.00	40.00	64.00
2.65	45.00	69.00
3.09	50.00	74.00
3.38	55.00	79.00
3.63	60.00	84.00
3.90	65.00	89.00
4.19	70.00	94.00
3.89	75.00	99.00
4.74	80.00	104.00
5.01	85.00	109.00

Table 2

Graph: Exp1.13

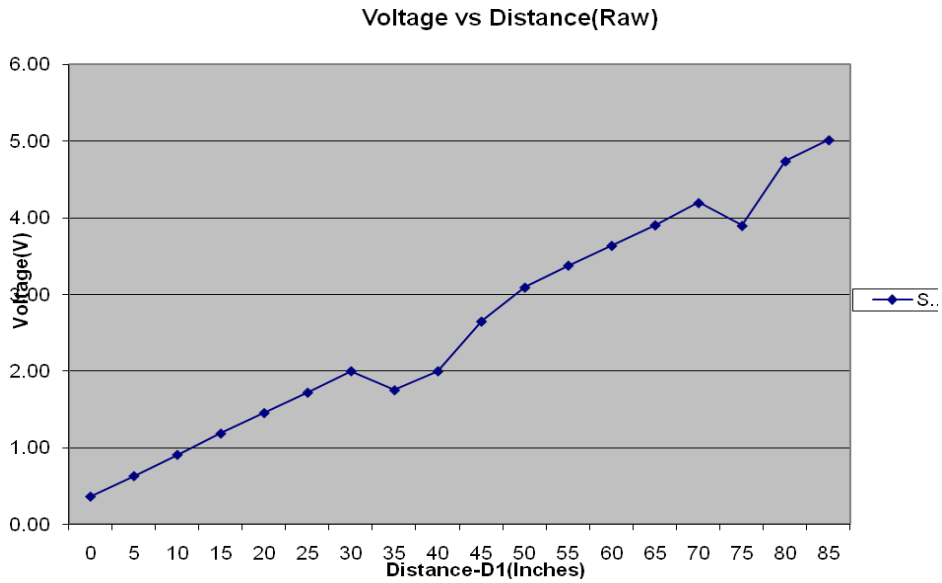

Fig. 12: Voltage vs Distance
The above Graph shows distances with standard deviation values which higher than the calculated tolerance value.

Further Instrumentation

After Run 1.13, Subsequent runs were aimed at eliminating interference from other reflecting surfaces around the sound field.
A conical attachment was built into the mount to reduce the interference.

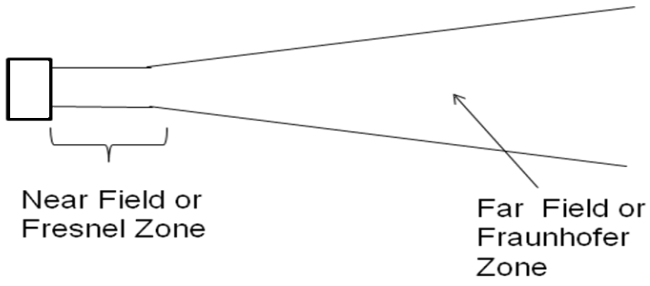

- Fresnel Zone Depth $=R^2/\lambda$
- (R = radius of the transducer)
- Construction of conical structure.

Fig 13: Sound wave Analysis

Run 1.20

Average Value	Std Dev	D1	D0	Delta
0.36	0.000023	0	24	
0.63	0.000028	5	39	0.27
0.91	0.000049	10	34	0.28
1.20	0.000066	15	39	0.28
1.45	0.000079	20	44	0.27
1.71	0.004681	25	49	0.26
2.00	0.000107	30	54	0.28
2.27	0.000133	35	59	0.27
2.55	0.000161	40	64	0.29
2.81	0.000189	45	69	0.26
3.10	0.000204	50	74	0.29
3.38	0.000214	55	79	0.28
3.60	0.000230	60	84	0.23
3.90	0.002185	65	89	0.30
4.19	0.001529	70	94	0.29
4.47	0.000299	75	99	0.28
4.76	0.000905	80	104	0.29
5.01	0.000309	85	109	0.26

Table 3
From the above results, average std. dev was shown to be in the order of 10^{-4}

Graph: Run 1.20

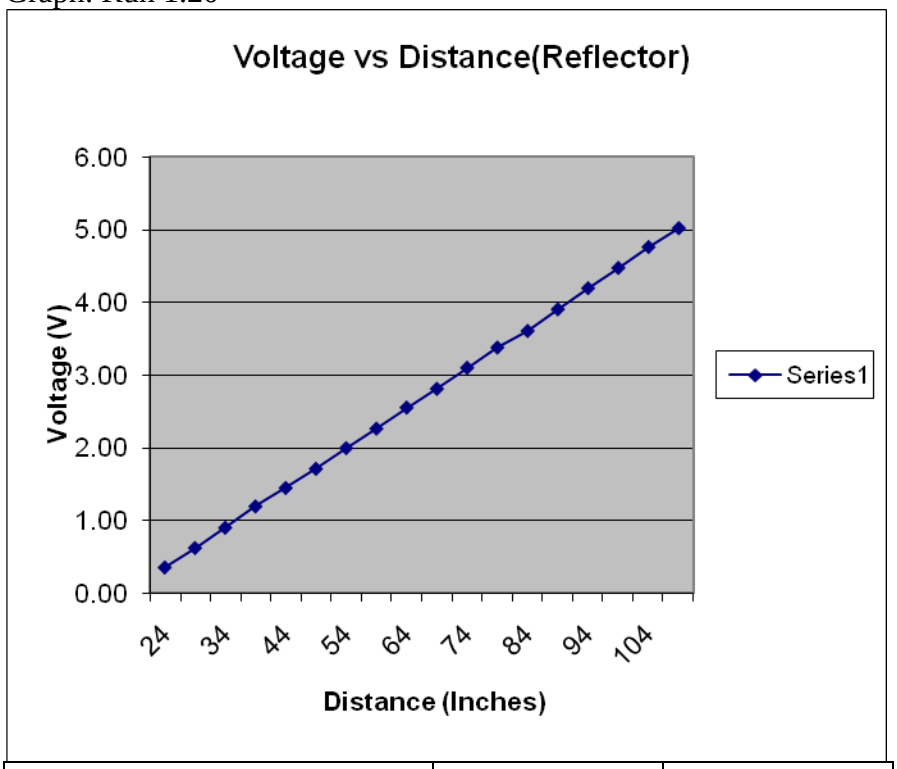

Temperature(T1)	72.83	73.26
Temperature(T2)	72.25	72.83
Ave Temperature	72.79	

Fig. 14 Voltage vs Distance

The above graph shows a plotting of voltage and distance (D1+D0) values after all other physical interference was removed from field. An average temperature of 72.79 ^{0}F was established using sensors placed at specific points within the field. This was then compared to our (D1+DO)/T measurements. Variations in our Voltage/Distance values with changing temperature in each run day remained consistent.

Data Processing

- **Labview**

The Labview software from National Instruments Inc. was used for our data collection. LabVIEW (Laboratory **V**irtual **I**nstrumentation **E**ngineering **W**orkbench) is a platform and development environment for a graphical programming language. It is commonly used for data acquisition, instrument control, and industrial automation. Execution is determined by the structure of a graphical block diagram on which the programmer connects different function nodes by drawing wires. These wires propagate variables and any node can execute as soon as all its input data become available. LabVIEW programs/subroutines are called virtual instruments (VI). Each VI has three components: a block diagram, a front panel, and a connector pane. A VI can either be run as a program with the front panel serving as a user interface or, when dropped as a node onto the block diagram, the front panel defines the inputs and outputs for the given node through the connector pane. The graphical approach also allows non-programmers to build programs simply by dragging and dropping virtual representations of lab equipment with which they are already familiar [1].

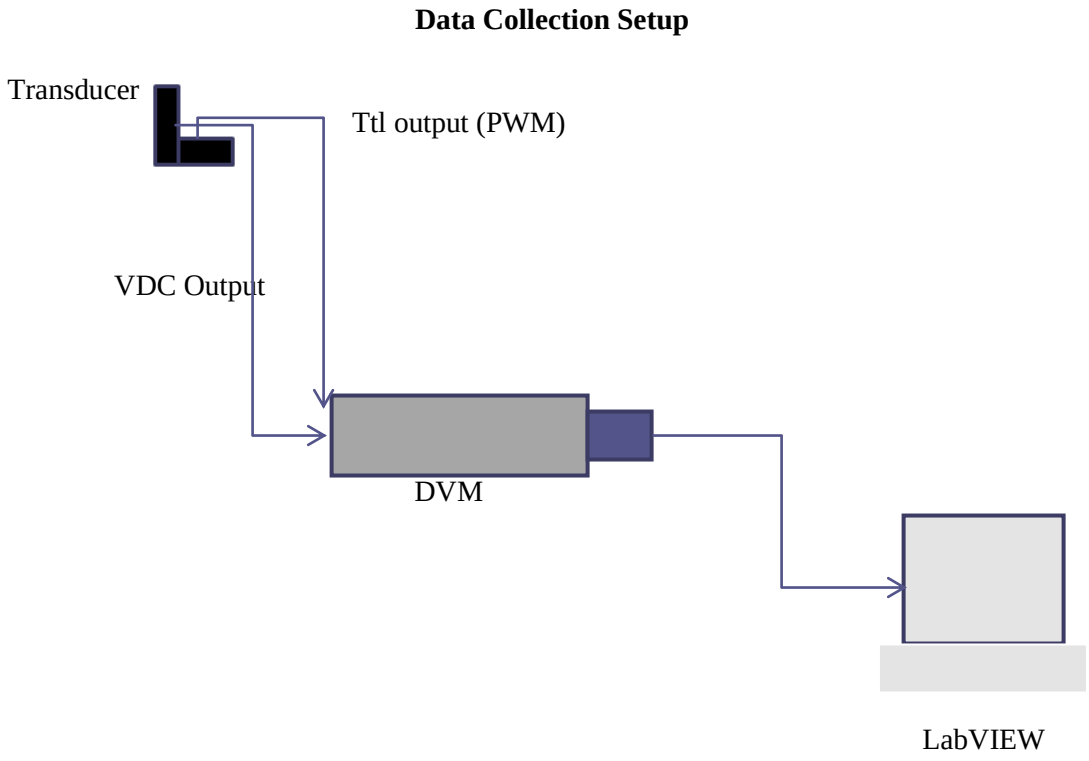

Fig. 15: Data Collection Setup

Block Diagrams

- Temperature-Dist Meas[1].vi

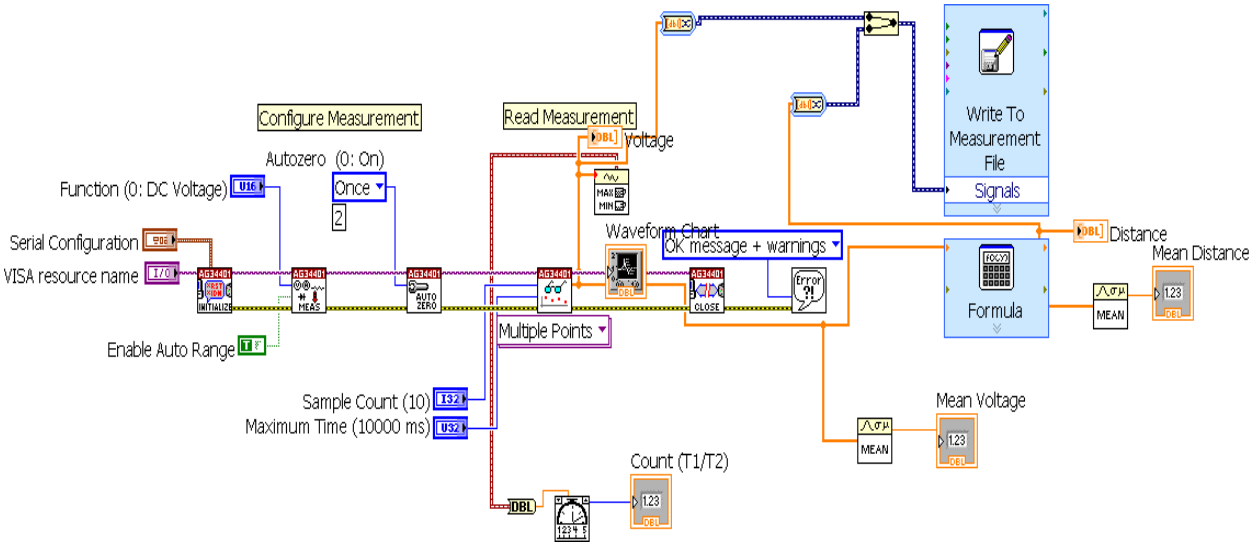

Fig. 16

- Temperature_Dist Meas [2].vi
  - A loop was put in place to monitor timing measurements
  - Future work to be done for accurate measurement of the PWM output

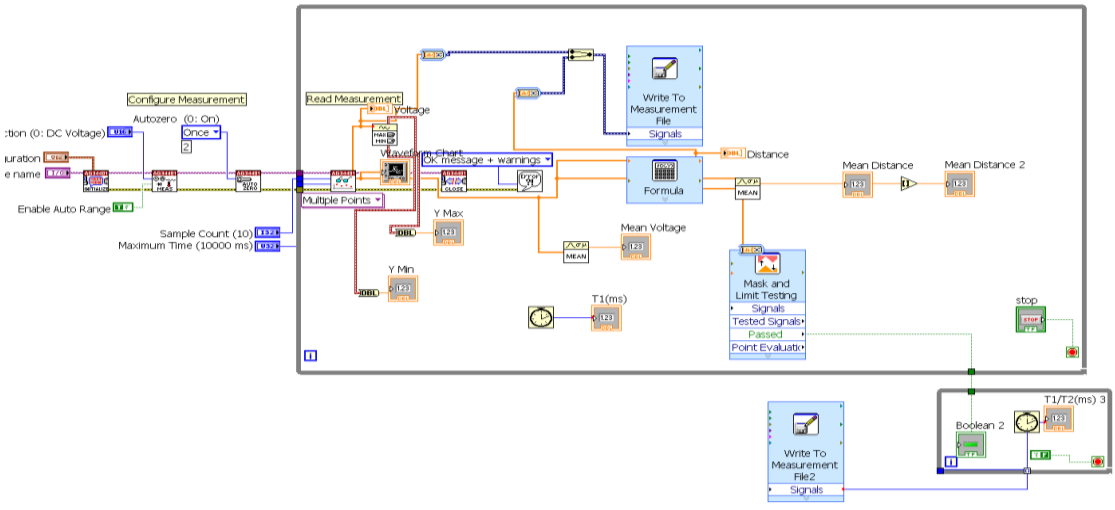

Fig. 17

Front Panels

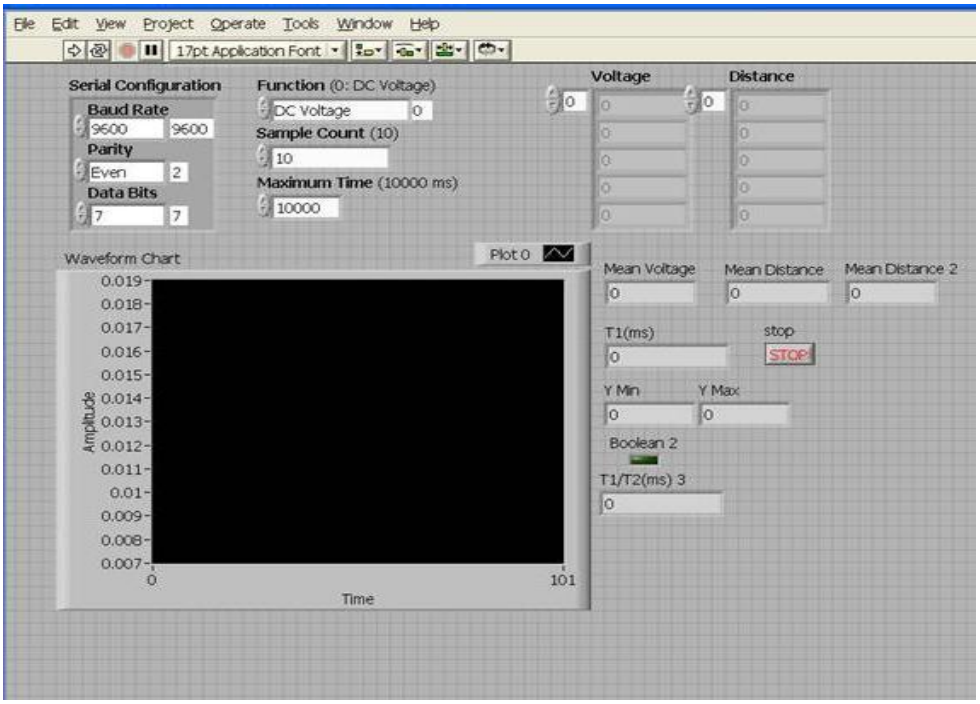

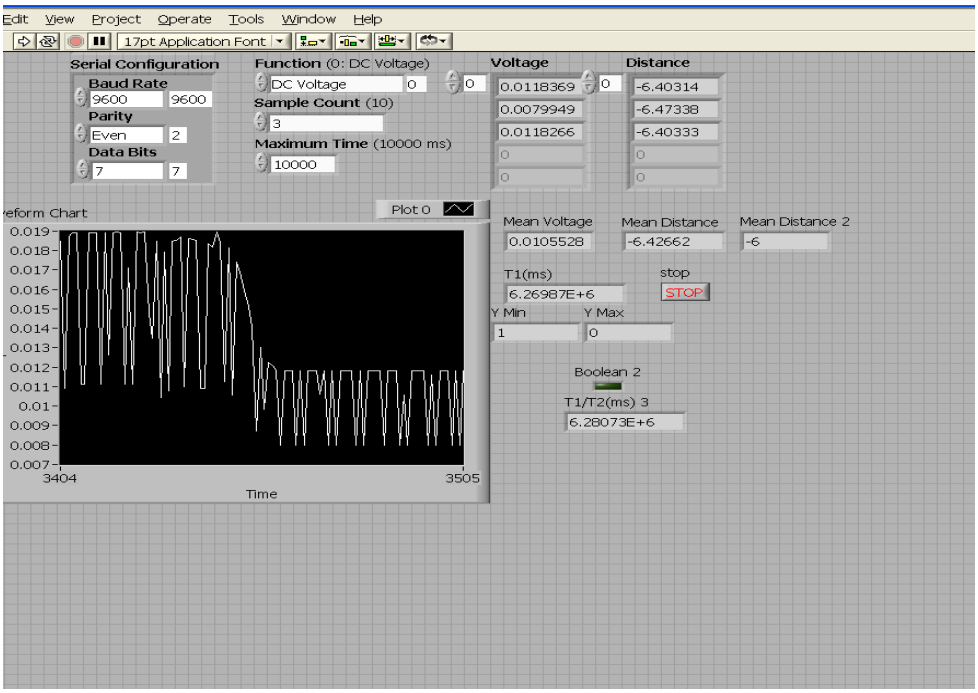

Fig. 18: Front Panels

Conclusion and Future Work

We have successfully calibrated voltage measurements to give us a value consistent with those from the System ’80 digital readout (Farrand Controls).
The transducer setup was redesigned and calibrated to give very accurate measurements to the scale of 10^{-4}m. The PWM output was optimally detected but will require a much faster DVM to accurately record the pulse width.

Further tests are required in an isolated chamber with VTC (Variable Temperature Control) capabilities. This will show the dependence of our speed of sound calculations on temperature alone and enable us to most accurately determine temperature change from the velocity of sound close to the path of the laser beam.

Acknowledgements

I would like to extend my gratitude to God for enabling me get this far in the project. I thank the Fermilab SIST program for offering me the opportunity to take part in this fulfilling research project, the Department of Energy and numerous researchers whose previous work served as a basis for a positive progression in the fulfillment my research goals. More thanks to the following:

- Horst Friedsam
- Jerry Zimmerman
- Dan Schoo
- Todd Johnson
- Gary Coppola

And

- The Entire Alignment and Metrology group for their training, help and support throughout the duration of the program

Works Cited

[1] NI LabVIEW – The Software That Powers Virtual Instrumentation. National Instruments Corporation. 7 Aug. 2008. http://www.ni.com/labview/

[2] How to Measure in Artificial Atmospheric Pressure Environments with Laser Trackers. Kevin Barron, Leica Geosystems (Metrology Division), Quality Magazine, March 1, 2007

[3] AIP Handbook of Condenser Microphones, Theory, Calibration and Measurements. George S. K. Wong; Tony F.W Embleton, AIP Press

[4] A new ultrasonic temperature measurement system for air conditioners in automobiles Teh-Lu Liao; Wen-Yuan Tsai; Chih-Feng Huang, Meas. Sci. Technol. **15** (2004) 413–419

[5] Mechanics, Heat and Sound, Isaac Maleh; Merrill Physical Science Series, Charles E. Merrill Pub. Company, 1969

[6] Ultrasonic Engineering, Julian R. Frederick; John Wiley and Sons Inc., New York.